

Reports

Wind Generation of the Costa Rica Dome

Abstract. *Upwelling in the Costa Rica Dome is seasonal and the result of the localized cyclonic wind stress curl. Fluctuations in the wind stress curl in the fall release the upwelled region as a Rossby wave. Similar low-latitude domes are hypothesized to be ubiquitous to those oceans where a localized cyclonic wind stress curl is associated with an Intertropical Convergence Zone.*

The Costa Rica Dome (1, 2) is a region of upwelling, 200 to 400 km in diameter, located in the eastern tropical Pacific Ocean near 8°N, 90°W. This area is situated at the eastern end of the thermocline ridge associated with the Equatorial Countercurrent (ECC) and received its name because the thermocline (3) in this region often reaches to within 10 m of the surface, forming a domelike feature. During the 1950's and 1960's several oceanographic surveys were conducted in the area of the Costa Rica Dome. The major portion of these observations were made during November, December, January, and February (4), but some observations were made at other times of the year (5). Because an upwelling feature always appeared in these data at the approximate location of the Costa Rica Dome, it was concluded that the dome must be permanent and stationary (1). It has been hypothesized (1) that upwelling in the dome is caused by the divergence produced by the northward turning of the ECC as it approaches the coast of

Central America. Upwelling velocities of 10^{-4} cm sec^{-1} have been computed from heat budget considerations for the Costa Rica Dome (1). The cyclonic circulation in the dome is thought to be (1) the result of three currents, the ECC to the south, the Costa Rica Coastal Current to the east, and the North Equatorial Current to the north, which come together off Costa Rica to form a cyclonic gyre.

Recently, a monthly data set of tropical Pacific wind stress has been constructed (6). This data set differs from earlier wind data sets in that it is on a 2° by 2° grid, which allows resolution of the smaller scale features in the atmospheric winds. It was while working with this data set that we noticed a feature in the wind field that led us to postulate that the Costa Rica Dome is actually a region of localized upwelling produced by the wind stress curl (6).

Initially, we used the wind stress data set to force a simple mass transport model (7) from which we obtained the gross, wind-driven circulation patterns

in the Pacific Ocean. Upon comparing the monthly stream-function maps, we found that the mass transport into the Costa Rica Dome region, due to the large-scale currents, is minimal. In support of this, geostrophic transport calculations (8) indicate that the transport of the ECC in this area is usually less than 10^7 $\text{m}^3 \text{sec}^{-1}$. Moreover, the calculated mass transport into this region is seasonal and reflects the north-south migration of the Intertropical Convergence Zone (ITCZ) (9). During the spring and early summer, flow into this region is not well developed, hence the mass transport into the Costa Rica Dome region is reduced (Fig. 1a). During the fall, the ECC intensifies, and there is a greater mass transport into the dome region (Fig. 1b). The mass transport streamlines (7) indicate a northward turning of the ECC as it nears the coast of Central America. The mass transport calculations are limited in that they are derived from a vertically integrated model which effectively masks upwelling. However, there is no indication of the permanent, cyclonic gyre in the Costa Rica Dome area required by the earlier hypothesis (1).

The negative result obtained from the mass transport calculation motivated us to look for another mechanism that could produce upwelling in the Costa Rica Dome region. As a starting point, we reexamined the results of a numerical model (10) developed to study the wind-driven equatorial current systems in the Pacific Ocean. The model contains linear dynamics on an equatorial β -plane and is forced by mean monthly winds (6). The model results that are of particular interest are the height fields from which the depth of the thermocline is estimated. Comparison of the monthly height field maps shows the development of upwelling in the Costa Rica Dome region during July (Fig. 2a). This upwelling persists throughout the summer and early fall. In November, the upwelled region is released as a Rossby wave (11) which propagates to the west (Fig. 2b). Maps of wind stress curl, derived from our wind stress data set, show that the Costa Rica Dome is in a region that corresponds to a maximum of the cyclonic (upwelling-favorable) wind stress curl (Fig. 3, a and b). It is this cyclonic wind stress curl that produces the localized upwelling.

During the late spring and early summer, in conjunction with the northward migration of the ITCZ, the cyclonic wind stress in the Costa Rica Dome region intensifies, thereby producing noticeable upwelling. The height field contours for July (Fig. 2a) indicate an upwelling re-

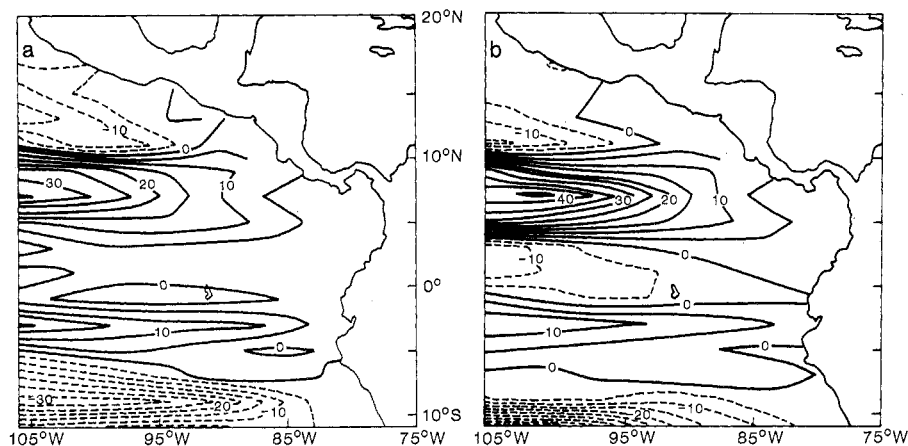


Fig. 1. Zonal mass transport in the Costa Rica Dome region for (a) July and (b) October. The contour interval is $5 \times 10^3 \text{ m}^2 \text{sec}^{-1}$. Solid lines indicate eastward transport.

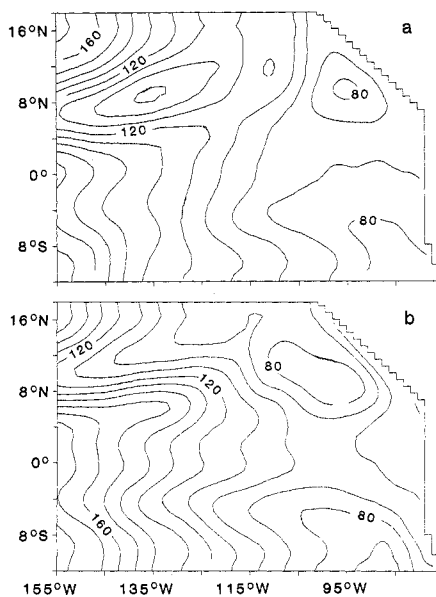


Fig. 2. Simulated upper-layer thickness for the Costa Rica Dome region for (a) July and (b) November. Data for the entire 12-month period are presented in (10). The y scale has been expanded to facilitate inspection of the plots. The contour interval is 10 m.

gion approximately 300 km in diameter extending from 89°W to 100°W and 7°N to 12°N. This upwelled region is larger than that described in (1). The thermocline displacements of 20 to 30 m agree with those observed in hydrographic data (4, 5). The magnitude of the maximum wind stress curl producing this upwelling is 10^{-8} dyne cm^{-3} (Fig. 3b), which, according to the vorticity equation, gives upwelling velocities of 10^{-4} cm sec^{-1} . This value agrees with earlier estimates of the vertical velocity derived from heat budget calculations (1).

During the fall, in conjunction with the southward movement of the ITCZ, the cyclonic wind stress curl over the Costa Rica Dome region weakens. Thus the upwelling is no longer balanced by the wind stress curl, and this imbalance releases the uplifted thermocline as a Rossby wave (Fig. 2b). In the linear numerical model, at 8°N to 10°N, low-frequency internal Rossby waves (11) propagate westward with theoretical phase speeds of 25 cm sec^{-1} . This westward movement is seen in the simulated height fields.

The Rossby wave is released during November when the ECC is strong (1). At this time, countercurrent velocities can approach 40 cm sec^{-1} (1), which causes the Rossby wave to appear to move to the east. This, combined with the northward flow of the Costa Rica Coastal Current, advects the Rossby wave to the northeast. Evidence for this

is found in hydrographic data collected during a survey of the Costa Rica Dome region in November and December 1959 (1). During the survey, an "eddy," which appeared to be moving to the northeast, was observed at 10°N, 88°W. This "eddy" was thought to be the result of fluctuations in the transport of the ECC (1). The spatial dimensions, thermocline elevation, and hydrographic properties associated with this feature lead us to conclude that it was actually a Rossby wave released from the upwelled region by the fluctuations in the wind stress curl. These advective effects are not observed in the numerical model results because the model is linear.

The hypothesis set forth in (1) to explain upwelling in the Costa Rica Dome is strongly dependent on the eastward flow of the ECC. However, upwelling has been observed in the dome during the spring and early summer when the ECC is not well developed (1, 5). Our wind stress data show that from May to October the Costa Rica Dome is influenced by upwelling-favorable wind stress curl (Fig. 3b). We believe that this is the mechanism responsible for upwelling in this region.

Earlier wind data sets were constructed on grids too large to resolve the cyclonic wind stress curl over the Costa Rica Dome region. Hence, wind forcing was dismissed as a causal mechanism for the observed upwelling in this area (1). The availability of wind stress maps with resolutions of 1° to 2° is of primary importance when studying the Costa Rica Dome region.

Further support for our hypothesis of upwelling due to the wind stress curl comes from the existence of a similar domed region off the west coast of Africa near 10°N (12). The pattern of wind forcing and the magnitude of the wind stress curl over this area are similar to those over the Costa Rica Dome region (6). The upwelling in this region cannot be attributed to influences from countercurrents, since the countercurrent in the eastern equatorial Atlantic is not very prominent (13). When the Atlantic Countercurrent is present, it has a southward component upon reaching the coast of Africa, the opposite of what occurs in the Pacific. A third dome is found at 10°S off the Indonesian coast in the Indian Ocean, the only other place in the world ocean where an ITCZ exists off an eastern boundary (14). This dome is made manifest between December and February when the ITCZ is situated south of Java.

The wind stress curl is a viable mecha-

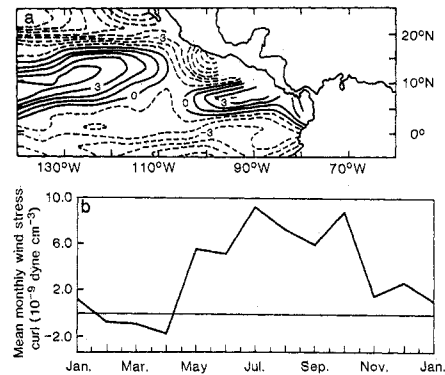


Fig. 3. (a) Mean annual wind stress curl (in 10^{-9} dyne cm^{-3}). Dashed lines are negative values. (b) Time series of the mean monthly wind stress curl at 10°N, 91°W. These maps are derived from a 10-year record of wind observations over the tropical Pacific Ocean.

nism for producing upwelling in the Costa Rica Dome region. At certain times of the year, this upwelling may be enhanced by the eastward flow of the ECC. Undercurrents may also be an important (15) influence on the upwelling, but this mechanism is not addressed here. Most of the observations of the dome have been made in the fall and winter. These data are neither synoptic nor sufficient to provide us with an understanding of the dynamics at work in this region. Clearly, the Costa Rica Dome is not a stationary feature, and more observations are necessary before we can discern the seasonal variability of this upwelling. Understanding of this variability would be of economic importance because the tuna fishery in the eastern tropical Pacific is related closely to the upwelling.

EILEEN E. HOFMANN*

ANTONIO J. BUSALACCHI

JAMES J. O'BRIEN

Departments of Meteorology and Oceanography, Florida State University, Tallahassee 32306

References and Notes

1. K. Wyrtki, *Fish. Bull.* **63**, 2 (1964).
2. W. W. Broenkow, *Limnol. Oceanogr.* **10** (1965); W. H. Thomas, *J. Mar. Res.* **37**, 2 (1979).
3. The thermocline is a region of steep vertical temperature gradient.
4. R. W. Holmes, *U.S. Fish Wildl. Serv. Spec. Sci. Rep. Fish.* **279** (1958); M. Blackburn, R. C. Griffiths, R. W. Holmes, W. H. Thomas, *U.S. Fish Wildl. Serv. Spec. Sci. Rep. Fish.* **420** (1962); Reference Report 60-20 (Scripps Institution of Oceanography, La Jolla, Calif., 1960); F. A. Richards, Technical Report 249 (University of Washington, Seattle, 1970); R. C. Dugdale and M. L. Healy, Technical Report 250 (University of Washington, Seattle, 1971).
5. R. W. Holmes and M. Blackburn, *U.S. Fish Wildl. Serv. Spec. Sci. Rep. Fish.* **345** (1960); W. S. Wooster and T. Cromwell, *Bull. Scripps Inst. Oceanogr.* **7**, 3 (1958).
6. The curl of the wind stress was calculated from 10 years (1961 to 1970) of monthly wind stress observations over the tropical Pacific. The original wind stress data [K. Wyrtki and G. Meyers, *J. Appl. Meteorol.* **15**, 698 (1976)] on a 2° latitude by 10° longitude grid were subjectively analyzed onto a 2° by 2° grid [S. B. Goldenberg and J. J.

O'Brien, *Mon. Weather Rev.* **109**, 1190 (1981)]. The finer resolution of the later study resulted in a finer resolution of the wind stress curl field. The areal extent and magnitude of prominent features of the eastern tropical Pacific wind stress curl are supported by the findings of S. Hastenrath and P. J. Lamb, *Climatic Atlas of the Tropical Atlantic and Eastern Pacific Oceans* (Univ. of Wisconsin Press, Madison, 1977). The climatic data presented by Hastenrath and Lamb are on a 1° by 1° grid, which covers the eastern tropical Pacific and tropical Atlantic oceans.

7. The mass transport model is given by $V = (1/\beta) \text{curl } \hat{\tau}$, where V is the meridional mass transport, β is the northward variation of the Coriolis parameter, and $\hat{\tau}$ is the wind stress vector. From the V transports and continuity

$$\frac{\delta U}{\delta x} + \frac{\delta V}{\delta y} = 0$$

considerations, the zonal mass transport, U , was calculated. The U and V mass transports were used to calculate streamlines from the model $\nabla^2 \psi = \xi$, where ψ is the stream-function and ξ is the mass transport vorticity

$$\frac{\delta V}{\delta x} - \frac{\delta U}{\delta y}$$

A streamline is a convenient scalar that can be used to visualize the vector mass transport field. The results of the mass transport calculations are presented in E. E. Hofmann and J. J. O'Brien, in preparation.

8. K. Wyrski and R. Kendall, *J. Geophys. Res.* **72**, 2073 (1967).
 9. The Intertropical Convergence Zone is the transition region between the northeast and southeast trade wind belts.
 10. A complete discussion of the model is given in A. J. Busalacchi and J. J. O'Brien, *J. Phys. Oceanogr.* **10**, 1929 (1980).
 11. Long-wavelength Rossby waves are long-period

oscillations that may be excited by fluctuations of the wind stress curl. The restoring force for these waves is the β effect, where β is $(\delta f/\delta y)$, f is the Coriolis acceleration, and y is the meridional direction. At the latitude of the Costa Rica Dome, the phase speed and group speed of these waves is $c_R = c^2/\beta y^2$, where c is the baroclinic phase speed and y is the distance from the equator. The presence of annual Rossby waves in the tropical North Pacific is not unique in this study. The vorticity equation has been used [G. Meyers, *J. Phys. Oceanogr.* **9**, 663 (1979)] to model the combined response of local Ekman pumping and Rossby waves. Analysis of observational data established that the largest annual variations in depth of the 14°C isotherm occur near 6°N and 12°N. The depth variations at 6°N were found to propagate westward at the speed of a nondispersive baroclinic Rossby wave. The results of Meyers' model correlated well with the observations at 6°N.

12. B. Voituriez and Y. Dandonneau, *Cah. ORSTOM Ser. Oceanogr.* **12**, 1 (1974).
 13. P. Tchernia, *Descriptive Regional Oceanography* (Marine Series vol. 3, Pergamon, New York, 1980), pp. 113-114.
 14. K. Wyrski, *Oceanographic Atlas of International Indian Ocean Expedition* (National Science Foundation, Washington, D.C., 1971).
 15. B. Voituriez, personal communication.
 16. We thank E-Chien Foo, J. M. Klinck, and C. N. K. Mooers for their helpful comments, J. Merritt for computer programming assistance, P. Teaf for typing, and two anonymous reviewers. This research was supported by NSF grant ATM-7920485 and Office of Naval Research-Selected Research Opportunities contract N00014-80-C-0076. Contribution No. 174 of the Geophysical Fluid Dynamics Institute at Florida State University and contribution No. 3 of the Pacific Equatorial Ocean Dynamics Program.
 * Present address: Department of Oceanography, Texas A&M University, College Station 77843.

23 December 1980; revised 3 August 1981

X-ray Absorption Spectroscopic Investigation of Trace Vanadium Sites in Coal

Abstract. *X-ray absorption spectroscopy was used to probe the chemical and structural environment of vanadium in coal. It was found that vanadium exists in at least two environments, in both of which it was coordinated to oxygens. There was no evidence of vanadium in nitrogen (porphyrin) or sulfide environments. It was also found that the vanadium environments in the raw coal did not survive unchanged in a liquefaction process. These findings have implications for coal cleaning processes and for trace element release into the liquefaction process stream.*

Coal contains nearly all the elements in the periodic table as impurities. Although the common inorganic elements in coal can be accounted for in the major minerals, the chemical and structural environments of many of the trace elements (those with a concentration ≤ 1000 ppm) cannot be confidently determined by conventional microscopic, spectroscopic, and diffraction techniques. An element that occurs in only a trace amount may, however, have a significant effect on coal conversion processes through its effects on corrosion, catalyst poisoning, and fugitive emissions. To deal rationally with these effects it is necessary to know the manner in which the element is held in coal and how its chemical environment changes during a process.

The average vanadium content of U.S.

coals is 20 ppm (1). However, the concentration in certain parts of some seams can be greater than 1500 ppm (2). Studies of coals by scanning electron microscopy and energy-dispersive x-ray analysis have found examples of vanadium-bearing silicates and iron pyrites (3). A number of density separation studies (4) have pointed to an organic environment for vanadium or a mixed organic-mineral environment. In an early study Triebs (5) found vanadyl porphyrin in a boghead coal. Vanadium is a well-known hot corrosion agent for metal parts (6) and has been identified as a factor in fibrogenesis affecting miners (7).

We took advantage of the unique atom selectivity of the x-ray absorption technique and used both the high-resolution near-edge K spectra and the extended x-ray absorption fine structure (EXAFS)

(8) to probe the local atomic environments of trace vanadium in coal. Intense synchrotron radiation was used as the x-ray source. The technique is nondestructive and requires no sample preparation that could disturb the elemental environments. It does not require a vacuum system and thus can be used with coal processing products such as liquids and tars, and it examines the whole sample, not just isolated regions.

The coal used in this study came from the top 15 cm of the Kentucky No. 9 seam. Parts of the seam are unusually high in vanadium. The vanadium concentrations in the samples ranged from 1000 to 1800 ppm. In addition to the raw coal, density-graded samples were prepared. The coal was pulverized under nitrogen in glass equipment to below a mesh size of 200 μm and centrifuged with Certigrav liquids. Two sets of samples were prepared, one lighter than 1.3 g/cm^3 and one heavier than 1.4 g/cm^3 . Samples of liquefied coal were also prepared. The pulverized coal was mixed with 1 percent (by weight) SnCl_2 and tetralin, then placed in a high-pressure bomb. The system was pressurized to 2000 pounds per square inch gauge with hydrogen, then heated to 300°C for 5 hours. At this time the coal had become plastic and tarry. Samples of the tarry product were used directly in the x-ray experiments.

The experiments were performed with the EXAFS-I-5 spectrometer (9) at the Synchrotron Radiation Laboratory at Stanford University during a dedicated run of SPEAR (the Stanford positron electron accelerator ring) at an electron energy of 3.0 GeV and a storage ring current of ~ 100 mA. The synchrotron x-ray beam from SPEAR was monochromatized with a channel-cut Si(220) crystal and a 1-mm entrance slit, which yielded a resolution of approximately 0.3 eV at the vanadium K edge at 5465 eV. Spectra of vanadium in coal were measured by the fluorescence EXAFS technique (10). This technique monitors the vanadium $K\alpha$ fluorescence intensity, which is proportional to the degree of absorption of the incident beam, and hence monitors the x-ray absorption spectrum. A fluorescence detector similar to that of Stern and Heald (11) was used. Spectral specimens were prepared by packing the powdered coal into Al cells 1500 μm thick equipped with 6- μm Kapton windows, which were sufficiently large that the x-ray beam impinged only on the coal sample. The cells were placed in a sample chamber purged with helium to minimize absorption and scat-